A LATIN computational strategy for multiphysics problems: Application to poroelasticity

David Dureisseix, Pierre Ladevèze, Bernard A. Schrefler

A LATIN computational strategy for multiphysics problems — application to poroelasticity

D. Dureisseix[1], P. Ladevèze[1] and B. A. Schrefler[2]

[1] LMT-Cachan (École Normale Supérieure de Cachan / CNRS / Université Paris 6), 61 Avenue du Président Wilson, F-94235 Cachan CEDEX, FRANCE
[2] Department of Structural and Transportation Engineering (University of Padova), Via Marzolo 9, 35131 Padova, ITALY

Abstract

Multiphysics phenomena and coupled-field problems usually lead to analyses which are computationally intensive. Strategies to keep the cost of these problems affordable are of special interest. For coupled fluid-structure problems, for instance, partitioned procedures and staggered algorithms are often preferred to direct analysis. In this paper, we describe a new strategy for solving coupled multiphysics problems which is built upon the LArge Time INcrement (LATIN) method. The proposed application concerns the consolidation of saturated porous soil, which is a strongly coupled fluid-solid problem. The goal of this paper is to discuss the efficiency of the proposed approach, especially when using an appropriate time-space approximation of the unknowns for the iterative resolution of the uncoupled global problem. The use of a set of radial loads as an adaptive approximation of the solution during iteration will be validated and a strategy for limiting the number of global resolutions will be tested on multiphysics problems.

This is the post-print accepted version of the following article: D. Dureisseix, P. Ladevèze, B. Schrefler, A LATIN computational strategy for multiphysics problems: Application to poroelasticity. *International Journal for Numerical Methods in Engineering* 56(10):1489-1510, Wiley-Blackwell, 2003, DOI: 10.1002/nme.622, which has been published in final form at http://http://onlinelibrary.wiley.com/doi/10.1002/nme.622/abstract

Keywords: multiphysics; coupled field; LATIN; porous media; fluid-structure interaction; consolidation

1 INTRODUCTION

Partitioned procedures and staggered algorithms [9, 8, 14, 16, 18, 21, 7] are often preferred (in the case of coupled fluid-structure problems, for instance) to direct analysis (also called the monolithic approach) from the point of view of computational efficiency. Moreover, partitioning strategies allow the use of different analyzers for different subsystems, thus helping to keep the software manageable.

Recently, a mixed domain decomposition method was developed for parallel computing environments [4]. A multi-level approach involving a homogenization procedure makes this method suitable for highly heterogeneous problems [13]. Here, we describe a new strategy for the resolution of coupled multiphysics problems: we use the LArge Time INcrement method (LATIN, see [12, 11]) to build a suitable approach by generalizing the concept of geometric interface between substructures to that of interface between different physics.

The LATIN method was originally developed for nonlinear time-dependent problems, such as plasticity and viscoplasticity problems. However, its concept has been successfully applied to dynamic problems, finite deformations, post-buckling analysis, etc. The LATIN method is a nonincremental iterative approach: at each iteration, the algorithm provides an approximation of the solution over the entire domain and the entire time interval considered. It is based on the following three principles:

- The first principle consists of separating the difficulties. For coupled-field problems, a first set of equations $\mathbf{A_d}$ contains the so-called admissibility conditions (compatibility of strains and pressure gradients, equilibrium and flow conservation). To avoid treating a global and a coupled problem simultaneously, the remaining equations are grouped into a separate set of equations $\mathbf{\Gamma}$ which are

local with respect to the space variables; usually, these are the constitutive relations describing the coupling between the fluid and the structure. In order to find the solution, i.e. the set of fields belonging to both $\mathbf{A_d}$ and $\mathbf{\Gamma}$, an iterative procedure is used.

- The second principle of the method consists of using search directions to build approximate solutions to $\mathbf{A_d}$ and to $\mathbf{\Gamma}$ alternatively until a sufficient level of convergence has been reached. Each iteration comprises 2 stages. The linear stage uses an initial search direction to provide an element of $\mathbf{A_d}$ once an element of $\mathbf{\Gamma}$ is known. This search direction is chosen in such a way that the structural and the fluid problems remain independent. Then, the local stage uses a second search direction, usually conjugate to the first, to find an element of $\mathbf{\Gamma}$, i.e. a solution which satisfies the coupling equations only locally in the domain.
- The third principle consists of using the fact that the successive approximations are defined over both the entire domain and the entire time interval in order to represent the solution in terms of a basis of radial loads.

Section 2 describes the reference problem. Section 3 describes the basic LATIN approach [6], while Section 4 validates the algorithm and compares it to another partitioned strategy. Section 5 proposes the use of an *ad hoc* approximation to search for the solution [5]. Finally, Section 6 concludes on the feasibility and the performance of the strategy.

2 THE REFERENCE PROBLEM

We consider the isothermal evolution over the time interval $[0,T]$ of a structure Ω made of a saturated porous material and subjected to small perturbations, see [21, 3]. The loading consists of a prescribed displacement $\underline{U}_d$ on part of the boundary $\partial_1\Omega$ and a traction force $\underline{F}_d$ on the complementary part $\partial_2\Omega$, plus a prescribed fluid pore pressure p_d on another part $\partial_3\Omega$ and, finally, a fluid flux on the complementary part $\partial_4\Omega$ of $\partial_3\Omega$ (see the example in Figure 1). For the sake of simplicity, no body forces $\underline{f}_d$ are considered.

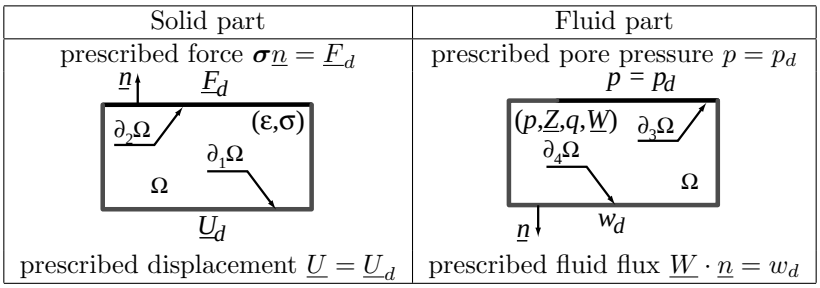

Figure 1: The reference problem

For solid entities, the strain is designated by $\boldsymbol{\varepsilon}$ and the stress by $\boldsymbol{\sigma}$. For fluid entities, the pore pressure gradient is designated by $\underline{Z}$, and, in order to have positive material characteristics, the notation $\underline{W}$ is used for the opposite of Darcy's velocity; finally, q designates the rate of accumulation of fluid in each representative elementary volume.

The state of the structure is described by the set of fields $\mathbf{s} = (\dot{\boldsymbol{\varepsilon}}, p, \underline{Z}, \boldsymbol{\sigma}, q, \underline{W})$ defined on the whole structure Ω and the time interval $[0,T]$ considered. The mathematical framework consists of searching the different fields in their respective spaces: $\underline{U} \in \mathcal{U}^{[0,T]}$, $\boldsymbol{\sigma} \in \mathcal{C}^{[0,T]}$, $p \in \mathcal{P}^{[0,T]}$, $q \in \mathcal{Q}^{[0,T]}$, $\underline{W} \in \mathcal{W}^{[0,T]}$; the problem is to find $\mathbf{s}$, in the corresponding space $\mathbf{S}^{[0,T]}$, which verifies at each time step:

- for the solid, stress equilibrium and strain compatibility:

$$\begin{aligned} \operatorname{div}\boldsymbol{\sigma} = 0 \quad \text{on } \Omega \quad \text{and} \quad \boldsymbol{\sigma}\underline{n} = \underline{F}_d \quad \text{on } \partial_2\Omega \\ \underline{U} \in \mathcal{U}^{[0,T]} \quad \text{and} \quad \boldsymbol{\varepsilon} = \boldsymbol{\varepsilon}(\underline{U}) \end{aligned} \tag{1}$$

  $\mathcal{U}^{[0,T]}$ being the set of finite-energy displacement fields on $\Omega\times[0,T]$ which are equal to $\underline{U}_d$ on $\partial_1\Omega$.

- for the fluid, flow conservation for Darcy's velocity $-\underline{W}$:

$$\begin{aligned} q = \operatorname{div}\underline{W} \quad \text{on } \Omega \quad \text{and} \quad \underline{W}\cdot\underline{n} = w_d \quad \text{on } \partial_4\Omega \\ \underline{Z} = \underline{\operatorname{grad}}\, p \quad \text{on } \Omega \quad \text{and} \quad p \in \mathcal{P}^{[0,T]} \end{aligned} \tag{2}$$

$\mathcal{P}^{[0,T]}$ being the set of finite-energy pressure fields on $\Omega \times [0,T]$, which are equal to p_d on $\partial_3\Omega$.

- the constitutive relations:
  - Hooke's law: the macroscopic stress $\boldsymbol{\sigma}$ is related to the strain $\boldsymbol{\varepsilon}$ and coupled with the pore pressure p so that:
$$\boldsymbol{\sigma} = \mathbf{D}\boldsymbol{\varepsilon} - bp\mathbf{1} \tag{3}$$
where $\mathbf{D}$ is Hooke's tensor of the drained skeleton and b is Biot's coefficient. The latter is obtained from the bulk moduli of the drained skeleton (or framework) K_t and of the solid phase (solid grains) K_s as $b = 1 - \frac{K_t}{K_s}$;
  - Darcy's law relates Darcy's velocity to the pore pressure gradient
$$\underline{W} = \frac{K}{\mu_w}\underline{Z} \tag{4}$$
K being the intrinsic macroscopic permeability and μ_w the dynamic viscosity of the saturation fluid. In all the following, the operator $\frac{K}{\mu_w}\mathbf{1}$ will be designated by $\mathbf{H}$;
  - the influence of compressibility relates the rate of fluid accumulation to the pressure rate and couples them with the rate of volume change:
$$q = \frac{1}{Q}\dot{p} + b\,\mathrm{Tr}\,\dot{\boldsymbol{\varepsilon}} \tag{5}$$
Q being Biot's modulus. For saturated soils, it is related to the porosity n and to the bulk moduli of the solid K_s and of the fluid K_w by: $\frac{1}{Q} = \frac{n}{K_w} + \frac{b-n}{K_s}$.

One can observe that if Biot's coefficient b equals 0, the solid problem and the fluid problem are uncoupled. For the steady-state problem, $\dot{p} = 0$, $\mathrm{Tr}\,\dot{\boldsymbol{\varepsilon}} = 0$, $q = 0$ and the two problems are partially uncoupled, since the fluid problem can be solved independently.

3 THE LATIN COMPUTATIONAL STRATEGY

The LArge Time INcrement method (LATIN, see [12]) is a nonincremental iterative approach originally developed for nonlinear time-dependent problems. However, its concept has been successfully applied to dynamic problems, post-buckling analysis, etc. At each iteration, this method produces an approximation of the solution on the whole domain and over the entire time interval considered. It is based on three principles of which the first two are briefly described in this section. For multiphysics problems, these two principles lead to a basic approach [6]. The last principle, whose use is required to gain high efficiency [5], will be described in Section 5.

3.1 Variational form of the reference problem

Let us first restate the reference problem using a variational formulation. The state of the structure $\mathbf{s}$ is governed by two sets of equations. The first set, designated by $\mathbf{A_d}$, contains the linear and uncoupled equations (possibly global over the entire structure): the so-called *admissibility* conditions (1,2). It consists, on the one hand, of $\underline{U} \in \mathcal{U}^{[0,T]}$ and $\boldsymbol{\sigma} \in \mathcal{C}^{[0,T]}$ such that:

$$\forall t \in [0,T], \quad \forall \underline{U}^\star \in \mathcal{U}_0, \quad \int_\Omega \mathrm{Tr}[\boldsymbol{\sigma}\boldsymbol{\varepsilon}(\underline{U}^\star)]d\Omega = \int_{\partial_2\Omega} \underline{F}_d \cdot \underline{U}^\star dS \tag{6}$$

where $\mathcal{U}_0$ is the set of finite-energy displacement fields on Ω which vanish on $\partial_1\Omega$. It also consists, on the other hand, of $p \in \mathcal{P}^{[0,T]}$, $q \in \mathcal{Q}^{[0,T]}$ and $\underline{W} \in \mathcal{W}^{[0,T]}$ such that:

$$\forall t \in [0,T], \quad \forall p^\star \in \mathcal{P}_0, \quad \int_\Omega (qp^\star + \underline{W} \cdot \underline{\mathrm{grad}}\, p^\star)d\Omega = \int_{\partial_4\Omega} w_d p^\star dS \tag{7}$$

where $\mathcal{P}_0$ is the set of finite-energy pressure fields on Ω which vanish on $\partial_3\Omega$.

Finally, the second set of equations, designated by $\boldsymbol{\Gamma}$, contains the equations which are local with respect to the space variables. This latter group of equations represents the constitutive relations (3,4,5)

which couple the solid and fluid fields locally in the domain. Since the reference problem is time-dependent, it requires initial conditions which are also chosen as belonging to $\mathbf{\Gamma}$.

Thus, the solution $\bar{\mathbf{s}}$ to the reference problem is $\bar{\mathbf{s}} = \mathbf{A_d} \cap \mathbf{\Gamma}$. The fundamental bilinear form on $\mathbf{S}^{[0,T]}$ is the following:

$$\langle \mathbf{s}, \mathbf{s}' \rangle = \int_0^T (1 - \frac{t}{T}) \int_\Omega (\mathrm{Tr}[\boldsymbol{\sigma} \dot{\boldsymbol{\varepsilon}}'] + \mathrm{Tr}[\boldsymbol{\sigma}' \dot{\boldsymbol{\varepsilon}}] + \underline{W} \cdot \underline{Z}' + \underline{W}' \cdot \underline{Z} + qp' + q'p) d\Omega dt$$

and its remarkable properties are:

- as long as $\mathbf{s}$, $\mathbf{s}'$ and $\mathbf{s}''$ belong to $\mathbf{A_d}$, $\langle \mathbf{s} - \mathbf{s}', \mathbf{s} - \mathbf{s}'' \rangle = 0$
- as long as $\mathbf{s}$ and $\mathbf{s}'$ belong to $\mathbf{\Gamma}$, $\langle \mathbf{s} - \mathbf{s}', \mathbf{s} - \mathbf{s}' \rangle \geq 0$

These properties, together with the positivity of the following parameters $(\mathbf{L}, \mathbf{H}, r)$ of the search directions, are needed to prove the convergence of the LATIN method. A general proof of convergence, even for non-linear problems, can be found in [12].

3.2 Separating the difficulties

The first principle of the LATIN method consists of avoiding the treatment of a global and a coupled problem simultaneously. Therefore, the solution to the problem is searched alternatively on $\mathbf{\Gamma}$ and on $\mathbf{A_d}$.

The second principle of the LATIN method uses an iterative procedure involving search directions. Recalling the main objective, which is to avoid treating a global and a coupled problem simultaneously, this step is performed with a specific choice for the search directions; this choice is also a feature of the LATIN method, see Figure 2.

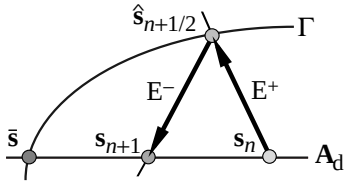

Figure 2: 2-stage LATIN iteration number $n+1$

3.3 A two-stage iterative strategy

Each iteration of the LATIN method contains 2 stages. In the linear stage, knowing an element of $\mathbf{\Gamma}$, we find an element of $\mathbf{A_d}$ using an initial search direction. In the local stage, we find an element of $\mathbf{\Gamma}$, i.e. a solution which verifies the coupling equations only locally in the domain, using a second search direction, usually conjugate to the previous one.

Local stage at iteration $n+1$. At this stage, the constitutive relations as well as the initial conditions are verified exactly. Once the previous stage has produced a solution $\mathbf{s}_n \in \mathbf{A_d}$, the problem is to find $\hat{\mathbf{s}}_{n+1/2} \in \mathbf{\Gamma}$. $\hat{\mathbf{s}}_{n+1/2} - \mathbf{s}_n$ must also lie on the search direction at the local stage:

$$\begin{aligned} (\hat{\boldsymbol{\sigma}}_{n+1/2} - \boldsymbol{\sigma}_n) + \mathbf{L}(\hat{\dot{\boldsymbol{\varepsilon}}}_{n+1/2} - \dot{\boldsymbol{\varepsilon}}_n) &= 0 \\ (\underline{\hat{W}}_{n+1/2} - \underline{W}_n) + \mathbf{H}(\underline{\hat{Z}}_{n+1/2} - \underline{Z}_n) &= 0 \\ (\hat{q}_{n+1/2} - q_n) + r(\hat{p}_{n+1/2} - p_n) &= 0 \end{aligned} \tag{8}$$

$\mathbf{L}$ and r are two parameters of the method; they do not modify the solution once convergence has been reached. However, their values modify the convergence rate of the algorithm. In a dimensional analysis, they can be chosen of the form:

$$\mathbf{L} = t_m \mathbf{D} \quad \text{and} \quad r = \frac{1}{Q t_h} \tag{9}$$

where t_m and t_h are two characteristic times.

With the constitutive relations (3,4,5), the local stage leads, at each integration point, to the resolution of a small ODE system which is local with respect to the space variable:

$$\begin{aligned} \mathbf{L}\dot{\hat{\boldsymbol{\varepsilon}}} + \mathbf{D}\hat{\boldsymbol{\varepsilon}} - b\hat{p}\mathbf{1} &= \mathbf{A}_n(t) \\ \frac{1}{Q}\dot{\hat{p}} + r\hat{p} + b\,\mathrm{Tr}\,\dot{\hat{\boldsymbol{\varepsilon}}} &= \alpha_n(t) \end{aligned} \tag{10}$$

where $\mathbf{A}_n = \boldsymbol{\sigma}_n + \mathbf{L}\dot{\boldsymbol{\varepsilon}}_n$ and $\alpha_n = q_n + rp_n$ are known quantities at the local stage $n+1$ and with the initial conditions on the pressure and the strain fields.

Linear stage at iteration $n+1$. Once $\hat{\mathbf{s}}_{n+1/2} \in \boldsymbol{\Gamma}$ is known, the linear stage consists of finding $\mathbf{s}_{n+1} \in \mathbf{A}_{\mathbf{d}}$. $\mathbf{s}_{n+1}$ must verify admissibility relations and is defined along a search direction conjugate to the previous one, so that the mechanical and the hydraulic problems remain uncoupled:

$$\begin{aligned} (\boldsymbol{\sigma}_{n+1} - \hat{\boldsymbol{\sigma}}_{n+1/2}) - \mathbf{L}(\dot{\boldsymbol{\varepsilon}}_{n+1} - \dot{\hat{\boldsymbol{\varepsilon}}}_{n+1/2}) &= 0 \\ (\underline{W}_{n+1} - \underline{\hat{W}}_{n+1/2}) - \mathbf{H}(\underline{Z}_{n+1} - \underline{\hat{Z}}_{n+1/2}) &= 0 \\ (q_{n+1} - \hat{q}_{n+1/2}) - r(p_{n+1} - \hat{p}_{n+1/2}) &= 0 \end{aligned} \tag{11}$$

The global yet uncoupled admissibility equations (6,7) must be solved by finite element discretization. Using the search direction, one obtains, on the one hand, the mechanical problem with the velocity $\underline{\dot{U}}$ as the unknown:

$$\forall t \in [0,T], \quad \forall \underline{U}^\star \in \mathcal{U}_0,$$
$$\int_\Omega \mathrm{Tr}[\boldsymbol{\varepsilon}(\underline{\dot{U}})\mathbf{L}\boldsymbol{\varepsilon}(\underline{U}^\star)]d\Omega = \int_\Omega \mathrm{Tr}[\hat{\mathbf{A}}_{n+1/2}(t)\boldsymbol{\varepsilon}(\underline{U}^\star)]d\Omega + \int_{\partial_2\Omega} \underline{F}_d \cdot \underline{U}^\star dS \tag{12}$$

$\hat{\mathbf{A}}_{n+1/2} = -\hat{\boldsymbol{\sigma}}_{n+1/2} + \mathbf{L}\dot{\hat{\boldsymbol{\varepsilon}}}_{n+1/2}$ being a known quantity when dealing with the solid part of the linear stage at iteration $n+1$.

One also obtains, on the other hand, the hydraulic problem with the pore pressure p as the unknown:

$$\forall t \in [0,T], \quad \forall p^\star \in \mathcal{P}_0,$$
$$\int_\Omega \underline{\mathrm{grad}}\, p \cdot \mathbf{H}\, \underline{\mathrm{grad}}\, p^\star d\Omega + \int_\Omega prp^\star d\Omega = \int_\Omega \hat{\alpha}_{n+1/2}(t)p^\star d\Omega + \int_{\partial_4\Omega} w_d p^\star dS \tag{13}$$

$\hat{\alpha}_{n+1/2} = -\hat{q}_{n+1/2} + r\hat{p}_{n+1/2}$ being also a known quantity at this stage.

Equations (12,13) are two uncoupled global problems with time t as parameter. Once $\dot{\boldsymbol{\varepsilon}}_{n+1} = \boldsymbol{\varepsilon}(\underline{\dot{U}})$ and p_{n+1} have been obtained, the search direction (11) is used to recover static quantities such as the stress field $\boldsymbol{\sigma}_{n+1}$ and the fluid accumulation q_{n+1}.

Error indicator for termination of the algorithm. Unlike classical incremental techniques, the LATIN method produces at each iteration an approximation of the solution over the entire structure Ω and the entire time interval $[0,T]$. Several error indicators can be used to stop the iterations, i.e. to decide when the solution is sufficiently accurate. For instance, one can use the error indicator based on the difference between an element $\mathbf{s}$ of $\mathbf{A}_{\mathbf{d}}$, and an element $\hat{\mathbf{s}}$ of $\boldsymbol{\Gamma}$:

$$\hat{\eta} = \frac{e(\hat{\mathbf{s}} - \mathbf{s})}{\frac{1}{2}e(\hat{\mathbf{s}} + \mathbf{s})} \tag{14}$$

with

$$e_t^2(\hat{\mathbf{s}} - \mathbf{s}) = \frac{1}{2}\|\hat{\boldsymbol{\varepsilon}} - \boldsymbol{\varepsilon}\|_{\mathbf{D}}^2 + \frac{1}{2}\|\hat{p} - p\|_{Q^{-1}}^2 \qquad e^2(\hat{\mathbf{s}} - \mathbf{s}) = \|e_t(\hat{\mathbf{s}} - \mathbf{s})\|_T^2$$
$$\|\boldsymbol{\varepsilon}\|_{\mathbf{D}}^2 = \int_\Omega \mathrm{Tr}[\boldsymbol{\varepsilon}\mathbf{D}\boldsymbol{\varepsilon}]d\Omega \qquad \|p\|_{Q^{-1}}^2 = \int_\Omega pQ^{-1}pd\Omega \qquad \|\alpha\|_T^2 = \int_0^T \alpha^2 dt$$

4 TEST CASE

4.1 Problem description and discretization

The proposed test case is the 2D plane strain problem described in Figure 3; it corresponds to the same boundary partition as in Figure 1. The time interval is $T = 36$ s, with $t_1 = T/10$ and the pressures are $p_1 = 1.54$ GPa and $p_d = 380$ MPa; the initial condition is $p(t = 0) = p_d$.

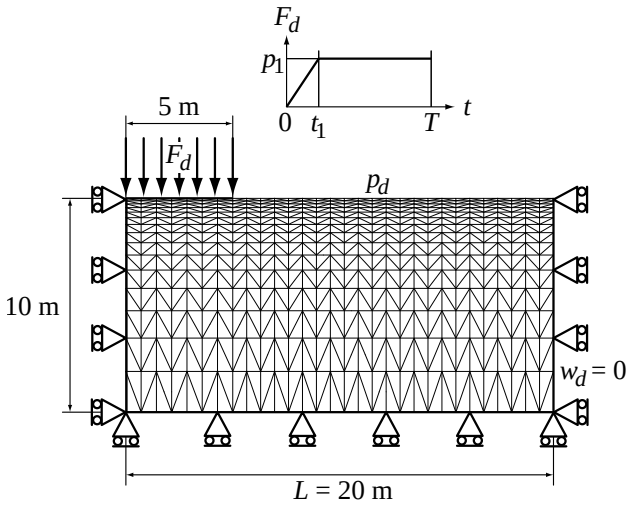

Figure 3: The test problem

The material characteristics in Table 1 correspond to a Berea sandstone and have been identified in [10]. Due to significant differences in the orders of magnitude of the material characteristics, an

Porosity	$n = 0.19$	Young's modulus	$E = 14.4$ GPa
Poisson's coeff.	$\nu = 0.2$	Biot's modulus	$Q = 13.5$ GPa
Biot's coeff.	$b = 0.78$	Permeability	$\frac{K}{\mu_w} = 2\ 10^{-10}\mathrm{m}^3.\mathrm{s.kg}^{-1}$

Table 1: water-saturated Berea sandstone poroelastic material characteristics

adimensionalization has been carried out.

The space discretization uses P2 elements (6-node triangles) for the displacement and P1 linear interpolation (also continuous throughout the elements) for the pore pressure, see [25, 2]. Seven Gauss points were used for the integration and the representation of field quantities such as those in $\mathbf{s}$, [26].

Concerning the time discretization, the time step chosen was $\Delta t = T/120$. The integration scheme used was the θ-method with a linear variation of the variables over a time step: $X_{i+1} = X_i + \Delta t \dot{X}_{i+\theta}$ (with the notation $\dot{X}_{i+\theta} = \theta \dot{X}_{i+1} + (1-\theta)\dot{X}_i$) and the associated derivation scheme was:

$$\dot{X}_{i+1} = \frac{1}{\theta \Delta t}(X_{i+1} - X_i) - \frac{1-\theta}{\theta}\dot{X}_i$$

The version used here was $\theta = 1$ (fully implicit).

In order to compare the proposed approach with the Iterated Standard Parallel Procedure (ISPP) described in [15], a reference solution was required. To produce that reference solution, we used the so-called direct monolithic scheme, which is briefly described below.

4.2 The monolithic solution scheme

The previous variational forms (6,7) along with the material behavior lead to the kinematic formulation of the 2-field problem with the displacement field and the pressure field as unknowns: $\underline{U} \in \mathcal{U}^{[0,T]}$, $p \in \mathcal{P}^{[0,T]}$

and $\forall t \in [0,T]$

$$\forall \underline{U}^\star \in \mathcal{U}_0, \quad \int_\Omega \mathrm{Tr}[\boldsymbol{\varepsilon}(\underline{U})\mathbf{D}\boldsymbol{\varepsilon}(\underline{U}^\star)]d\Omega - \int_\Omega bp\,\mathrm{Tr}\,\boldsymbol{\varepsilon}(\underline{U}^\star)d\Omega = \int_{\partial_2\Omega} \underline{F}_d \cdot \underline{U}^\star dS$$

$$\forall p^\star \in \mathcal{P}_0, \quad \int_\Omega \underline{\mathrm{grad}}\, p \cdot \mathbf{H}\, \underline{\mathrm{grad}}\, p^\star d\Omega + \int_\Omega \dot{p}\frac{1}{Q}p^\star d\Omega + \int_\Omega bp^\star\,\mathrm{Tr}\,\dot{\boldsymbol{\varepsilon}} d\Omega = \int_{\partial_4\Omega} w_d p^\star dS$$

Using the previous space discretization, this leads to the coupled global system of equations at each time step:

$$\begin{aligned} KU - Np &= f_d \\ Hp + S\dot{p} + N^T\dot{U} &= g_d \end{aligned}$$

K, H and S are the stiffness, permeability and compressibility matrices; N is the coupling term, f_d are the generalized forces corresponding to $\underline{F}_d$ and g_d is the generalized flux corresponding to w_d. The previous formulation is symmetrized by derivating the first group of equations with respect to time, leading to:

$$\begin{bmatrix} K & -N \\ -N^T & -S \end{bmatrix} \begin{bmatrix} \dot{U} \\ \dot{p} \end{bmatrix} + \begin{bmatrix} 0 & 0 \\ 0 & -H \end{bmatrix} \begin{bmatrix} U \\ p \end{bmatrix} = \begin{bmatrix} \dot{f}_d \\ -g_d \end{bmatrix}$$

With the same integration scheme, this diffusion-type incremental problem at time step t_{i+1} is:

$$\begin{bmatrix} K & -N \\ -N^T & -S - \theta\Delta t H \end{bmatrix} \begin{bmatrix} U \\ p \end{bmatrix}_{i+1} = C_i \tag{15}$$

with the given right-hand side:

$$C_i = \Delta t \begin{bmatrix} \dot{f}_d \\ -g_d \end{bmatrix}_{i+\theta} + \begin{bmatrix} K & -N \\ -N^T & -S + (1-\theta)\Delta t H \end{bmatrix} \begin{bmatrix} U \\ p \end{bmatrix}_i$$

Note that the iteration matrix depends on the time step Δt; even for a linear problem, the use of a variable time step requires some refactorization of this matrix. The cost increase for a direct coupled simulation is also apparent on this matrix: it is due, on the one hand, to the number of degrees of freedom, which include both the displacement and the pore pressure unknowns, and, on the other hand, to the increase in bandwidth, even with a good renumbering scheme.

The time interval studied corresponds effectively to the transient part of the soil response: Figure 4 shows the evolution of the maximum pore pressure over the time interval $[0,T]$.

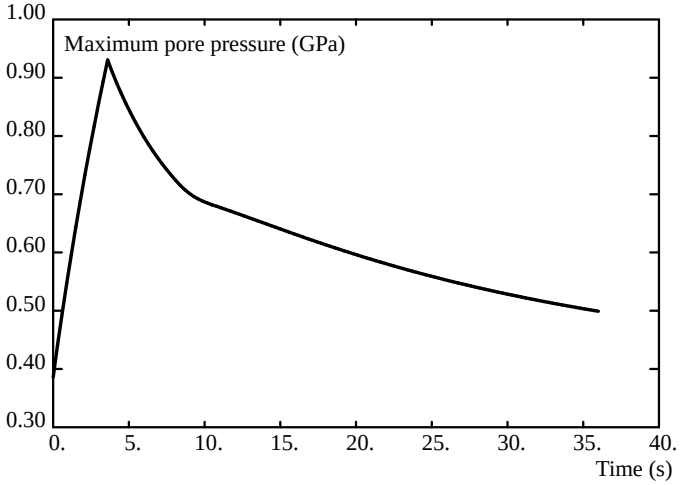

Figure 4: Maximum pore pressure for the transient evolution

4.3 Iterated Standard Parallel Procedure

This section briefly recalls the ISPP strategy [15], in order to compare it to the LATIN strategy.

Using the so-called monolithic formulation (15), the scheme consists of partitioning the iteration matrix, in Gauss-Seidel fashion, into diagonal and off-diagonal blocks (coupling terms). Using the predictor

$$\begin{bmatrix} U \\ p \end{bmatrix}_{i+1}^{p} = \begin{bmatrix} U \\ p \end{bmatrix}_{i}$$

the uncoupled partitioned problem is:

$$\begin{bmatrix} K & 0 \\ 0 & -S - \theta \Delta t H \end{bmatrix} \begin{bmatrix} U \\ p \end{bmatrix}_{i+1} = \begin{bmatrix} 0 & N \\ N^T & 0 \end{bmatrix} \begin{bmatrix} U \\ p \end{bmatrix}_{i+1}^{p} + C_i \tag{16}$$

Convergence is achieved by subiterations using the new evaluation of the solution at t_{i+1} as the new predictor; this is required to recover the consistency of the scheme. With an inconsistent scheme, keeping the mesh size constant while reducing the time step would cause the algorithm to converge toward an incorrect solution (see, for instance, [22]).

Another interesting property of a partitioned scheme is its unconditional stability. It is possible to stabilize several schemes with dedicated techniques, such as in [17, 24], or by condensing one type of unknown onto the others; (for further description see, for instance, [15, 20]). These latter techniques suffer from high computational cost because of the condensation step which destroys the sparsity of the operators. Finally, a good convergence rate is a key to computational efficiency.

Typically, the ISPP scheme is a consistent, yet conditionally stable, algorithm. To improve convergence of this fixed-point method with strong coupling, one needs to apply relaxation at each subcycle, transforming the Gauss-Seidel technique into a Successive OverRelaxation (SOR) technique (see, for instance, [1]).

The method's parameters are the number of subiterations n_{sub} and the relaxation parameter ω.

4.4 First results and comparison

The monolithic approach, the ISPP and the LATIN method were all implemented into the industrial FE code Cast3M (formerly Castem 2000) [23] developed at the CEA in Saclay, France. To compare a given solution $\mathbf{s}$ obtained using the LATIN method or the ISPP with the reference solution $\bar{\mathbf{s}}$ obtained using the monolithic incremental approach, the following error was used:

$$\eta(\mathbf{s}) = \frac{e(\mathbf{s} - \bar{\mathbf{s}})}{e(\bar{\mathbf{s}})}$$

As a first test, the calculation was performed using the LATIN method without time-space representation of the unknowns. The search direction parameters (9) were optimized and set to $t_m = 0.015 t_c$ and $t_h = 0.030 t_c$, where t_c is a characteristic time obtained from dimensional analysis: $t_c = L^2/(QH)$ where L is the width of the structure. In the present example, $t_c = 148$ s.

Figure 5 shows the influence of the choice of the parameters on the convergence rate, with the evolution of the previous error η versus iteration number n_{it}. It is more sensitive to the fluid parameter t_h than the solid one t_m. As a good search direction cannot be chosen in practise by testing the convergence this way, an automatic evaluation of the parameters t_m and t_h would be of interest. Either a physical interpretation of these parameters or a numerical study of the convergence rate could tune the values of t_m and t_h.

With the same discretization as for the monolithic approach, a linear stage of the LATIN method consists of solving, at each time step t_i, the two independent problems (12,13):

$$\begin{aligned} L\dot{U}_i &= B_u^T \hat{\mathbf{A}}_i + f_{di} \\ [H + R] p_i &= B_p^T \hat{\alpha}_i + g_{di} \end{aligned}$$

Matrices L and R arise from the search directions and, with the particular form (9), one gets $L = t_m K$ and $R = \frac{1}{t_h} S$. Note that the time step Δt does not appear on the left-hand sides; therefore, each of the matrices L and $[H + R]$ requires only one factorization, whether an adaptive time step is used or not. Finally, the right-hand sides are calculated in such a way that:

$$U^T B_u^T \hat{\mathbf{A}} = \int_\Omega \text{Tr}[\hat{\mathbf{A}} \boldsymbol{\varepsilon}(\underline{U})] d\Omega \qquad \text{and} \qquad p^T B_p^T \hat{\alpha} = \int_\Omega \hat{\alpha} p d\Omega$$

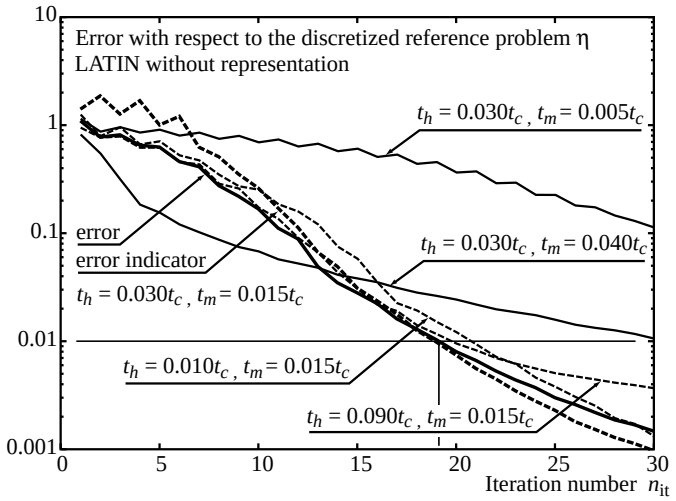

Figure 5: Convergence of the LATIN method without representation

The local stage is performed by integrating in time the small ODE system (10) at each Gauss point of each element.

Concerning the ISPP, Figure 6 shows the influence of the relaxation parameter ω, with the evolution of the error η versus the number of subcyclings per time step n_{sub}. At each subcyclings, the ISPP solves the two independent problems in (16). In this test case, a constant time step is used, so the left hand side is only factorized once. An optimum value exists near $\omega = 0.5$, whereas large values (close to 1) impair convergence.

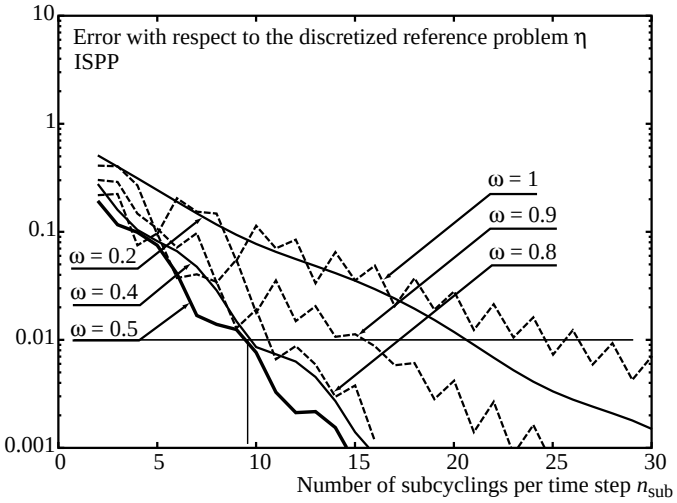

Figure 6: Convergence of the ISPP

To compare the optimal cases for the LATIN method and the ISPP, one has to notice that in both cases, the number of uncoupled global resolutions is equal to the iteration number n_{it} or the subcyclings number n_{sub} multiplied by the number of time steps (120 in this example) for the solid part as well as for the fluid part. For this example, the number of global, linear and uncoupled resolutions needed to achieve a given level of accuracy of the solution is about twice for the LATIN method that required by the ISSP approach.

This result validates the feasibility of the proposed approach, but the efficiency is not good enough for this strategy to be competitive. To achieve better efficiency, the third principle of the LATIN method, described in the next section, is required.

5 REPRESENTATION OF THE UNKNOWNS

The third principle of the LATIN method concerns the use of an appropriate, mechanics-based representation of the unknowns (for instance, the superimposition of radial loads used also for plasticity and viscoplasticity problems). This last principle is required to achieve high computational efficiency, see [12]. This section describes the use of such a representation in multiphysics problems and its potential efficiency. The example presented in the next section was used to validate this approach.

The unknowns of $\mathbf{A_d}$ are sought in the form of sums of products of a scalar time function by a field which depends only on the space variables. For instance, the strain rate is approximated by $\dot{\boldsymbol{\varepsilon}}(M,t) = v_0(t)\boldsymbol{\varepsilon}(\underline{V}_0) + \sum_j v_j(t)\boldsymbol{\varepsilon}(\underline{V}_j)$, where the pairs $(v_k(t), \underline{V}_k(M))$ must be determined automatically by the algorithm. Throughout the iterations, additional pairs may be added if necessary for accuracy; otherwise, the current space vectors $\underline{V}_k$ remain unchanged and only the time functions v_k are updated. For this purpose, a preliminary stage must be added to the algorithm before the linear stage is applied. In either case, at iteration $n+1$, a correction to the previous approximation must be determined, i.e.: $\mathbf{s}_{n+1} = \mathbf{s}_n + \Delta\mathbf{s}$.

A first version of this principle is described below. It consists of using a representation for the admissible kinematic corrections while the static corrections are calculated along the search direction. Consequently, the static quantities are not strictly admissible unless convergence has been reached. Computing admissible static quantities would require an additional numerical effort [12].

5.1 Linear stage with representation at iteration $n+1$

The objective of this stage is to add one pair (for the sake of simplicity) to the previous set of radial loads which represents the kinematic unknowns.

Solid part. The *strain correction* is sought in the approximate form $\Delta\dot{\boldsymbol{\varepsilon}} = v\boldsymbol{\varepsilon}(\underline{V})$, where $v(t)$ is a scalar time function and $\underline{V}(M) \in \mathcal{U}_0$. In order to determine the pair $(v, \underline{V})$ uniquely, a normalization is enforced, e.g. $\|\boldsymbol{\varepsilon}(\underline{V})\|^2_{\mathbf{L}} = 1$. Once the strain correction has been obtained, the stress is computed along the search direction (11):

$$\boldsymbol{\sigma} = \mathbf{L}\dot{\boldsymbol{\varepsilon}}_{n+1} - \hat{\mathbf{A}}_{n+1/2} = \mathbf{L}\Delta\dot{\boldsymbol{\varepsilon}} - \Delta\hat{\mathbf{A}} \quad \text{with} \quad \Delta\hat{\mathbf{A}} = \hat{\mathbf{A}}_{n+1/2} - \mathbf{L}\dot{\boldsymbol{\varepsilon}}_n$$

Let us recall that $\hat{\mathbf{A}}_{n+1/2} = -\hat{\boldsymbol{\sigma}}_{n+1/2} + \mathbf{L}\hat{\dot{\boldsymbol{\varepsilon}}}_{n+1/2}$ is a known quantity at this stage.

The unknown pair $(v, \underline{V})$ is sought such that the stress is weakly admissible, i.e.:

$$\forall \underline{U}^\star = v^\star\underline{V} + v\underline{V}^\star \in \mathcal{U}_0^{[0,T]}, \quad \int_0^T\int_\Omega \mathrm{Tr}[\boldsymbol{\sigma}\boldsymbol{\varepsilon}(\underline{U}^\star)]d\Omega dt = \int_0^T\int_{\partial_2\Omega} \underline{F}_d\cdot\underline{U}^\star dSdt$$

With the proposed normalization, $(v, \underline{V})$ is such that:

$$v_{|_t} = \int_\Omega \mathrm{Tr}[\Delta\hat{\mathbf{A}}\boldsymbol{\varepsilon}(\underline{V})]d\Omega + \int_{\partial_2\Omega}\underline{F}_d\cdot\underline{V}dS$$

$$\forall \underline{V}^\star \in \mathcal{U}_0, \quad \int_\Omega \mathrm{Tr}[\boldsymbol{\varepsilon}(\underline{V})\mathbf{L}\boldsymbol{\varepsilon}(\underline{V}^\star)]d\Omega = \int_0^T \frac{v}{\|v\|_T^2}\left(\int_\Omega \mathrm{Tr}[\Delta\hat{\mathbf{A}}\boldsymbol{\varepsilon}(\underline{V}^\star)]d\Omega + \int_{\partial_2\Omega}\underline{F}_d\cdot\underline{V}^\star dS\right)dt$$

This coupled system of equations is solved with a fixed-point method and the number of substeps is usually small. The global system is no more solved at each time step, but only once for each given weighting time function $v(t)$.

Once discretized in space, these equations become:

$$V^T L V = 1 \tag{17}$$

$$v_{|_t} = V^T(B_u^T\Delta\hat{\mathbf{A}} + f_d) \tag{18}$$

$$LV = \int_0^T \frac{v}{\|v\|_T^2}(B_u^T\Delta\hat{\mathbf{A}} + f_d)dt \tag{19}$$

where superscript T designates transposition and, as previously, $B_u^T\Delta\hat{\mathbf{A}}$ are the generalized forces that balance the field $\Delta\hat{\mathbf{A}}$. The usual initial guess for the time function in order to initialize the fixed point is the error indicator in time from the previous iteration. Several indicators may be used to stop the

fixed point. For instance, one can monitor the stationarity of the fixed-point method: if $(v_0, \underline{V}_0)$ is the previous pair and $(v, \underline{V})$ the current pair, an appropriate indicator is:

$$\xi^2 = \frac{\frac{1}{2}\int_0^T \|v\boldsymbol{\varepsilon}(\underline{V}) - v_0\boldsymbol{\varepsilon}(\underline{V}_0)\|^2_{\mathbf{L}} dt}{\frac{1}{2}\int_0^T \|v\boldsymbol{\varepsilon}(\underline{V})\|^2_{\mathbf{L}} dt} = \frac{\frac{1}{2}(\|v\|^2_T + \|v_0\|^2_T) - \int_0^T v v_0 dt V_0^T L V}{\frac{1}{2}\|v\|^2_T}$$

The algorithm corresponding to the solid linear stage is described in Table 2.

Calculate the right-hand side	$\hat{f} \leftarrow B_u^T(\mathbf{L}\hat{\boldsymbol{\varepsilon}}_{n+1/2} - \hat{\boldsymbol{\sigma}}_{n+1/2} - \mathbf{L}\dot{\boldsymbol{\varepsilon}}_n) + f_d$
Initialize the time function	$v \leftarrow \|\hat{\boldsymbol{\varepsilon}}_{n+1/2} - \boldsymbol{\varepsilon}_n\|_{\mathbf{L}}$
Loop on the fixed point	
Solve	$LV = \int_0^T \frac{v}{\|v\|^2_T}\hat{f}dt = \tilde{f}$
Normalize	$\beta \leftarrow (\tilde{f}^T V)^{1/2}$
	$V \leftarrow \beta^{-1}V$
	$v \leftarrow \beta v$
Stopping criteria	for the pair (v, V)
Recalculate the time function	$v \leftarrow V^T\hat{f}$
End of loop	

Table 2: The solid linear stage algorithm at iteration $n+1$

Fluid part. The previous scheme for the solid part of the multiphysics problem must be extended to the hydraulic components $(p, \underline{Z})$ and $(q, \underline{W})$ in the same way.

For instance, the *pressure correction* has the following approximate expression: $\Delta p = \pi P$ and $\Delta\underline{Z} = \pi\,\underline{\text{grad}}\,P$, where $\pi(t)$ is a scalar time function and $P(M) \in \mathcal{P}_0$. This time, the useful normalization is $\|P\|^2_r + \|\,\underline{\text{grad}}\,P\|^2_{\mathbf{H}} = 1$.

The corresponding static unknowns are obtained with the search direction (11):

$$\underline{W} = (\underline{\hat{W}}_{n+1/2} - \mathbf{H}\underline{\hat{Z}}_{n+1/2}) + \mathbf{H}\underline{Z}_{n+1} = \mathbf{H}\underline{Z}_{n+1} = \mathbf{H}\Delta\underline{Z} + \mathbf{H}\underline{Z}_n$$
$$q = rp_{n+1} - \hat{\alpha}_{n+1/2} = r\Delta p - \hat{\alpha}_{n+1/2} + rp_n$$

Let us recall that $\hat{\alpha}_{n+1/2} = -\hat{q}_{n+1/2} + r\hat{p}_{n+1/2}$ is a known quantity at this stage.

The best pair (π, P) is the one which achieves weak static admissibility:

$$\forall p^\star = \pi^\star P + \pi P^\star \in \mathcal{P}_0^{[0,T]}, \quad \int_0^T \int_\Omega (\underline{W} \cdot \underline{\text{grad}}\, p^\star + q p^\star) d\Omega dt = \int_0^T \int_{\partial_4\Omega} w_d p^\star dS dt$$

With the proposed normalization, (π, P) is such that:

$$\pi_{|_t} = \int_{\partial_4\Omega} w_d P dS + \int_\Omega (\hat{\alpha}_{n+1/2} - rp_n) P d\Omega - \int_\Omega \underline{Z}_n \mathbf{H}\,\underline{\text{grad}}\, P d\Omega$$

and

$$\forall P^\star \in \mathcal{P}^0, \quad \int_\Omega (PrP^\star + \underline{\text{grad}}\, P \cdot \mathbf{H}\,\underline{\text{grad}}\, P^\star) d\Omega =$$
$$= \int_0^T \frac{\pi}{\|\pi\|^2_T} \left(\int_{\partial_4\Omega} w_d P^\star dS + \int_\Omega (\hat{\alpha}_{n+1/2} - rp_n) P^\star d\Omega - \int_\Omega \underline{Z}_n \mathbf{H}\,\underline{\text{grad}}\, P^\star d\Omega \right) dt$$

This can be solved with another fixed-point method. Using spatial discretization, the problem to be solved is:

$$P^T[H+R]P = 1 \tag{20}$$
$$\pi = P^T(B_p^T\hat{\alpha}_{n+1/2} - [H+R]p_n + g_d) \tag{21}$$
$$[H+R]P = \int_0^T \frac{\pi}{\|\pi\|^2_T}(B_p^T\hat{\alpha}_{n+1/2} - [H+R]p_n + g_d)dt \tag{22}$$

As previously, $B_p^T\hat{\alpha}_{n+1/2}$ is the generalized flux that balances the field $\hat{\alpha}_{n+1/2}$. Both the initialization and the termination criteria are similar to the previous ones.

The algorithm for the fluid linear stage described in Table 3 is very similar to its solid counterpart.

Calculate the right-hand side	$\hat{g} \leftarrow B_p^T(r\hat{p}_{n+1/2} - \hat{q}_{n+1/2}) - [H+R]p_n + g_d$
Initialize the time function	$\pi \leftarrow \|\hat{p}_{n+1/2} - p_n\|_{Q^{-1}}$
Loop on the fixed point	
Solve	$[H+R]P = \int_0^T \frac{\pi}{\|\pi\|_T^2}\hat{g}dt = \tilde{g}$
Normalize	$\beta \leftarrow (\tilde{g}^T P)^{1/2}$
	$P \leftarrow \beta^{-1}P$
	$\pi \leftarrow \beta\pi$
Stopping criteria	for the pair (π, P)
Recalculate the time function	$\pi \leftarrow P^T\hat{g}$
End of loop	

Table 3: The fluid linear stage algorithm at iteration $n+1$

Efficiency of the representations. The space fields are determined by solving a small number of global systems (19,22) (within the fixed-point subiterations), while the time functions are calculated by integrating a small number of differential equations (moreover, in the linear case treated here, these equations are explicit (18,21)). If the convergence rate is similar to that of the case without representation, significant performance improvement can be expected. This will be illustrated on the example of the following section.

In order to prevent degeneration of the sets of space fields, orthonormalization may be performed so that $V_i^T L V_j = \delta_{ij}$ for the solid fields and $P_i^T[H+R]P_j = \delta_{ij}$ for the fluid fields. During this orthonormalization process, if the latest fields generated are too dependent on the previous ones, they may be skipped.

5.2 Initial solution

To start the algorithm using the same kind of representation for $\mathbf{s}_0$, let us observe that this initial solution can be represented as the superimposition of as many radial loads as there are loading parameters.

Indeed, if (for the sake of simplicity) the loading depends on only one parameter, i.e. if $\underline{F}_d = \lambda(t)\underline{F}(M)$ and $w_d = \gamma(t)G(M)$, the initial solution for the solid part is obtained with $\dot{\underline{U}} = v_0(t)\underline{V}_0(M) \in \mathcal{U}^{[0,T]}$ and

$$\forall t \in [0,T], \quad \forall \underline{V}^\star \in \mathcal{U}_0, \quad \int_\Omega \mathrm{Tr}[\boldsymbol{\varepsilon}(\dot{\underline{U}})\mathbf{L}\boldsymbol{\varepsilon}(\underline{V}^\star)]d\Omega = \int_{\partial_2\Omega} \lambda \underline{F}\cdot\underline{V}^\star dS$$

Therefore, $v_0 = \lambda$ and $LV_0 = f$, where f are the generalized forces corresponding to $\underline{F}$.

Then, $\boldsymbol{\sigma}_0 = v_0\mathbf{L}\boldsymbol{\varepsilon}(\underline{V}_0)$. Let us note that since there are as many pairs as there are loading parameters the initial stress field is statically admissible.

The initial solution for the fluid part is obtained with $p = \pi_0 P_0 \in \mathcal{P}^{[0,T]}$ and

$$\forall t \in [0,T], \quad \forall P^\star \in \mathcal{P}_0, \quad \int_\Omega (prP^\star + \underline{\mathrm{grad}}\, p \cdot \mathbf{H}\,\underline{\mathrm{grad}}\, P^\star)d\Omega = \int_{\partial_4\Omega} \gamma G P^\star dS$$

Therefore, $\pi_0 = \gamma$ and $[H+R]P_0 = g$, where g is the generalized flux corresponding to G.

Similarly, $\underline{W}_0 = \pi_0 \mathbf{H}\,\underline{\mathrm{grad}}\, P_0$ and $q_0 = \pi_0 r P_0$ are statically admissible.

5.3 Preliminary stage at iteration $n+1$

The objective of the preliminary stage is to update the time functions of the various representations. This stage is much simpler if the space functions are orthogonalized each time a new space function is added to the previous set.

The idea is to re-use the space fields already generated during the previous iterations as much as possible. Such a procedure is similar to the one consisting in the re-use of Krylov subspaces to accelerate the convergence of the successive resolutions, see [19] for instance, as in Newton-Krylov methods.

Strain correction. In the preliminary stage, the update is sought through a correction of the form $\Delta\dot{\boldsymbol{\varepsilon}} = \sum_j w_j \boldsymbol{\varepsilon}(\underline{V}_j)$, where w_j are the time functions to be determined while $\underline{V}_j$, at this stage, are known.

As noted above, if the space fields are orthonormalized, i.e. if $V_j^T L V_k = \delta_{jk}$, the unknown time functions are solutions of the uncoupled system:

$$w_j = V_j^T (B_u^T \Delta \hat{\mathbf{A}} + f_d)$$

An equivalent scheme is to recalculate the time functions directly, i.e. $v_j + w_j$, instead of their correction. In this case, the problem is to have $\sum_j v_j \mathbf{L}\dot{\boldsymbol{\varepsilon}}(\underline{V}_j) - \hat{\mathbf{A}}_{n+1/2}$ weakly homogeneously admissible; this leads to:

$$v_j = V_j^T B_u^T \hat{\mathbf{A}}_{n+1/2}$$

Pressure correction. The update for the fluid part is also sought through a correction of the form $\Delta p = \sum_j \mu_j P_j$, where μ_j are the time functions to be determined whereas P_j are known at this stage. Once again, if the space fields are orthonormalized, i.e. if $P_j^T [H + R] P_k = \delta_{jk}$, the unknown time functions are solutions of the uncoupled system:

$$\mu_j = P_j^T (B_p^T \hat{\alpha}_{n+1/2} - [H + R] p_n + g_d)$$

The same remark as for the solid part applies: the problem is equivalent to modifying the time functions with:

$$\pi_j = P_j^T B_p^T \hat{\alpha}_{n+1/2}$$

6 EXAMPLE AND COMPARISON OF EFFICIENCIES

Let us consider again the plane strain problem of Section 4. With the proposed representation, the algorithm is modified as described in Table 4.

Solid initialization	solve a global mechanical problem to get (v_0, V_0)
Fluid initialization	solve a global hydraulic problem to get (π_0, P_0)
Loop on iterations	
Local stage	solve the local differential systems to get $(\hat{\boldsymbol{\varepsilon}}, \hat{\boldsymbol{\sigma}})$, $(\hat{p}, \hat{q})$
Stopping criteria	compute error indicators
Solid preliminary stage	update time functions v_j
If a new pair is required	
Solid linear stage	fixed point on the global mechanical problem to get (v, V)
Orthonormalization	modification of (v, V) and time functions v_j
End if	
Fluid preliminary stage	update time functions π_j
If a new pair is required	
Fluid linear stage	fixed point on the global hydraulic problem to get (π, P)
Orthonormalization	modification of (π, P) and time functions π_j
End if	
End of loop	

Table 4: The LATIN algorithm for multiphysics problem

In this test, the time-space representation of the admissible fields was added and, this time, solid and fluid linear stages always followed the preliminary stage. In other terms, at each iteration, one spatial field was added to the previous set for the solid part and one for the fluid part. Moreover, the number of fixed-point subiterations for each linear stage was set to 1; in this case, only one global mechanical problem and one global hydraulic problem were solved at each iteration. The same search direction parameters were used for this test case, as for the previous one.

Figure 7 shows the evolution of the error when such a representation is used compared to the previous case without representation. For this situation, using a representation does not impair the convergence rate at all. Thus, the representation is well-suited to this kind of problem. Throughout the following discussion, the number of subiterations is kept equal to 1 (only one global resolution for the fluid and one for the solid at each iteration).

In order to avoid the generation of worthless space functions, a criterion based on the efficiency of the preliminary step can be used. If the preliminary stage reduces the error with respect to the previous

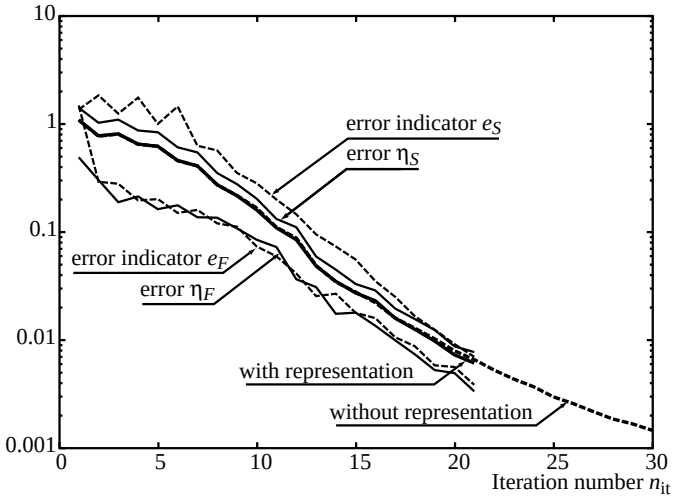

Figure 7: Evolution of the error and error indicators with the LATIN approach

iteration significantly, one can expect that adding a new space function is not necessary. The error estimations provide such information. At iteration n, $\tilde{s}_n$ designates the solution immediately after the preliminary stages and s_n the solution after the linear stages (if such stages are performed). The relevant indicators are designated by $\tilde{e}_n^S$, $\tilde{e}_n^F$, e_n^S and e_n^F, where superscripts 'S' and 'F' stand for the solid part and the fluid part respectively:

$$\left(\tilde{e}_n^S\right)^2 = \frac{\int_0^T \|\tilde{\boldsymbol{\varepsilon}}_n - \hat{\boldsymbol{\varepsilon}}_{n-1/2}\|^2_{\mathbf{D}} dt}{\frac{1}{2}\int_0^T \|\tilde{\boldsymbol{\varepsilon}}_n + \hat{\boldsymbol{\varepsilon}}_{n-1/2}\|^2_{\mathbf{D}} dt} \qquad \left(\tilde{e}_n^F\right)^2 = \frac{\int_0^T \|\tilde{p}_n - \hat{p}_{n-1/2}\|^2_{Q^{-1}} dt}{\frac{1}{2}\int_0^T \|\tilde{p}_n + \hat{p}_{n-1/2}\|^2_{Q^{-1}} dt}$$

$$\left(e_n^S\right)^2 = \frac{\int_0^T \|\boldsymbol{\varepsilon}_n - \hat{\boldsymbol{\varepsilon}}_{n-1/2}\|^2_{\mathbf{D}} dt}{\frac{1}{2}\int_0^T \|\boldsymbol{\varepsilon}_n + \hat{\boldsymbol{\varepsilon}}_{n-1/2}\|^2_{\mathbf{D}} dt} \qquad \left(e_n^F\right)^2 = \frac{\int_0^T \|p_n - \hat{p}_{n-1/2}\|^2_{Q^{-1}} dt}{\frac{1}{2}\int_0^T \|p_n + \hat{p}_{n-1/2}\|^2_{Q^{-1}} dt}$$

Every time $\dfrac{\tilde{e}_n^S}{e_{n-1}^S} < \zeta$ the solid linear stage may be skipped. In the same way, if $\dfrac{\tilde{e}_n^F}{e_{n-1}^F} < \zeta$, the fluid linear stage may be skipped, see Figure 8. Figure 7 also shows the evolution of these various error indicators with the previous representation of the unknowns. The errors with respect to the reference solution η^S (for the solid) and η^F (for the fluid) are derived in the same way.

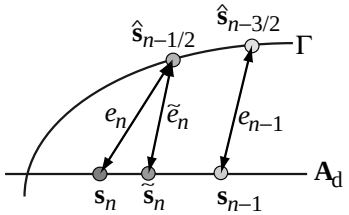

Figure 8: Indicators at iteration n

The overall results are illustrated in Figure 9, which shows the evolution of the error vs. iterations. Since the cost of the global mechanical problem and the cost of the global hydraulic problem are not the same, Figure 10 displays the error as a function of the number of strain space fields generated n_S and as a function of the number of pore pressure fields generated n_F for different values of the threshold ζ. In the most interesting case, when $\zeta = 0.8$, only 8 global mechanical resolutions and 16 global hydraulic resolutions are required to get an error η less than 1%. If $\zeta = 0$, i.e. if one pair for each physics is added at each iteration, 18 global resolutions are required for each physics. In comparison, the basic algorithm with no representation requires 18×120 global resolutions for the solid part and the same number for the fluid part in order to get the same accuracy, whereas the ISPP scheme requires 9×120 resolutions. Thus, in terms of number of global resolutions, there is a ratio of 90. Of course, there are other costs in the algorithm than those related to global resolutions, but for large-scale problems these tend to

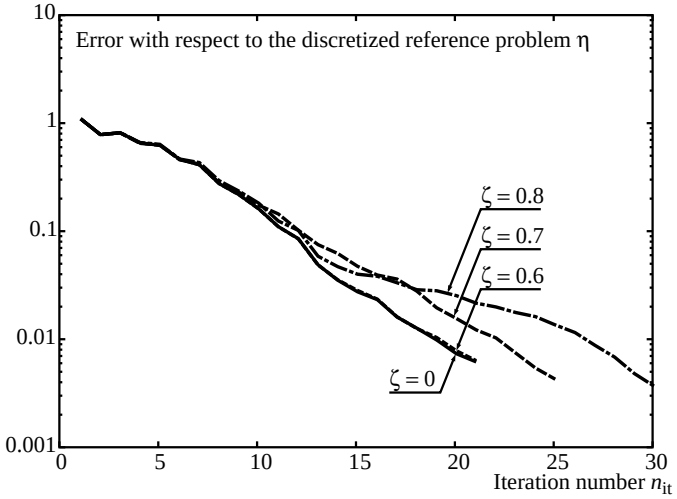

Figure 9: Evolution of the error for several thresholds ζ

b	ISPP	LATIN ($\zeta = 0$)	LATIN ($\zeta = 0.8$)		
	n_{sub}	$n_{\text{it}} = n_S = n_F$	n_{it}	n_S	n_F
0.25	6	19	20	4	9
0.5	8	18	20	6	10
0.75	9	19	26	9	13
0.9	10	20	22	7	13
1	13	21	21	8	12

Table 5: Comparative costs for the ISPP (with $\omega = 0.5$), and with the LATIN method (with $t_m = 0.015t_c$ and $t_h = 0.030t_c$) versus Biot's coefficient b

dominate. Nevertheless, it would be interesting to perform a complexity analysis to quantify these costs more precisely.

The last test concerns the behaviour of the approaches with respect to the coupling coefficient b. Table 5 shows the number of subcyclings for the ISPP, and the number of space fields for the LATIN method, to reach convergence ($\eta \leq 1$ %). The cost of the ISPP clearly increases when the coupling is stronger. As the LATIN is somehow a self-adaptive strategy, the cost does not follow so clearly the coupling and is almost constant.

7 CONCLUSION

On the example above, using the basic LATIN approach with no mechanics-based approximation to solve the linear stage over the entire domain and the entire time interval, the number of global, linear uncoupled resolutions needed to achieve a given level of solution accuracy was about twice that required by the ISSP approach.

In this paper, the time-space approximation is tested and appears to be well suited to multiphysics problems. Since the use of such an approximation did not influence the convergence rate of the proposed algorithm, the efficiency was significantly improved, particularly with the adjunction of a strategy to limit the number of global resolutions. The number of constitutive relation integrations is always greater than with the ISSP scheme, but these involve only local computations at each integration point. Thus, the proposed strategy appears to be competitive from an efficiency point a view.

Nevertheless, other improvements, such as the automatic determination of the search direction parameters, would be welcome. The coupling between two different codes (one for each physical problem) can be developed extensively. The ability for the codes to exchange only the few pairs representing the solution during the iterative process seems attractive in that it reduces the amount of information interchange.

Let us also mention that, for problems involving only the solid part, a micro-macro multiscale computational strategy based on the LATIN method has proved to be efficient [13], especially for heterogeneous

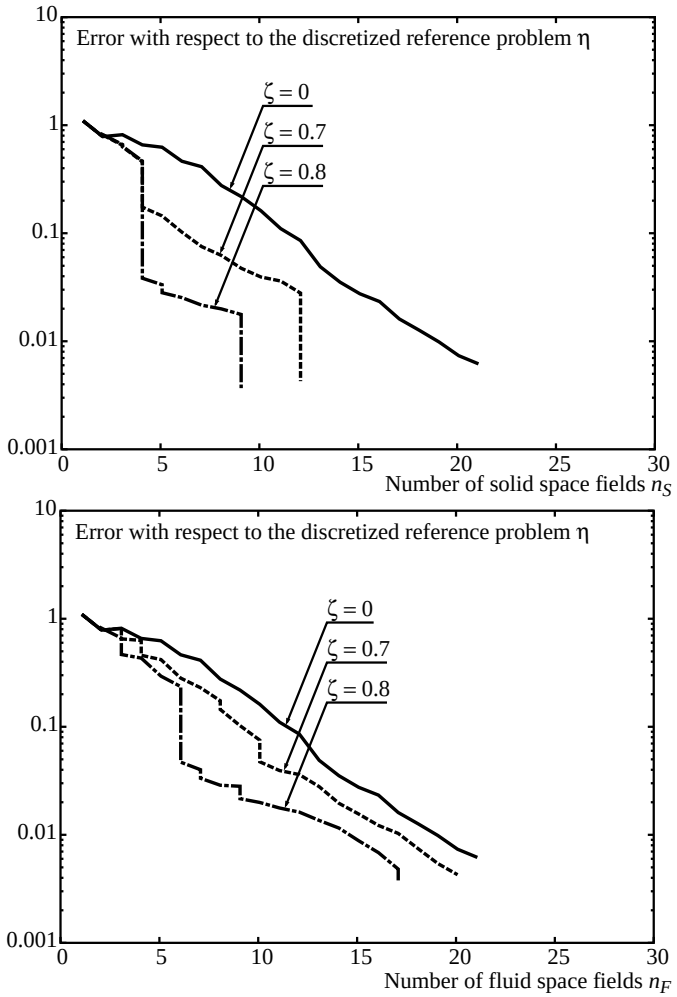

Figure 10: Evolution of the error versus the number of space fields generated

structures; it features a multilevel mixed domain decomposition method involving an automatic homogenization procedure as a global problem. The splitting used in this paper for multiphysics problems is concerned only with an "interface" between the physics, while the micro-macro approach uses geometric interfaces between substructures. Such an approach could be easily applied both for the solid and for the fluid, independently. Then, a more efficient strategy, suited to parallel architecture computers, could be derived from the present multiphysics strategy and the micro-macro approach.

References

[1] R. Barrett, M. Berry, T. F. Chan, J. Demmel, J. Donato, J. Dongarra, V. Eijkhout, R. Pozo, C. Romine, and H. V. der Vorst. *Templates for the Solution of Linear Systems: Building Blocks for Iterative Methods*. SIAM, 1994.

[2] F. Brezzi and M. Fortin. *Mixed and Hybrid Finite Element Methods*, volume 15 of *Computational Mathematics*. Springer, 1991.

[3] O. Coussy. *Mechanics of porous continua*. John Wiley & Sons, 1995.

[4] D. Dureisseix and P. Ladevèze. *A multi-level and mixed domain decomposition approach for structural analysis*, volume 218 of *Contemporary Mathematics, Domain Decomposition Methods 10*, pages 246–253. AMS, 1998.

[5] D. Dureisseix, P. Ladevèze, and B. A. Schrefler. LATIN computational strategy for multiphysics problems. In *Proceedings of the 2nd European Conference on Computational Mechanics (ECCM)*, 2001.

[6] D. Dureisseix, P. Ladevèze, and B. A. Schrefler. LATIN strategy for coupled fluid-solid problems in the domain. In K. J. Bathe, editor, *Proceedings of the First M.I.T. Conference on Computational Fluid and Solid Mechanics*, pages 1143–1146. Elsevier, 2001.

[7] C. Farhat and M. Lesoinne. Two efficient staggered algorithms for the serial and parallel solution of three-dimensional nonlinear transient aeroelastic problems. *Computer Methods in Applied Mechanics and Engineering*, 182:499–515, 2000.

[8] C. A. Felippa and T. L. Geers. Partitioned analysis for coupled mechanical systems. *Engineering Computation*, 5:123–133, 1988.

[9] C. A. Felippa and K. C. Park. Staggered transient analysis procedures for coupled mechanical systems: formulation. *Computer Methods in Applied Mechanics and Engineering*, 24:61–111, 1980.

[10] GRECO. Scientific report, GRECO Géomatériaux, 1990.

[11] P. Ladevèze. Sur une famille d'algorithmes en mécanique des structures. In *Comptes-Rendus de l'Académie des Sciences*, volume 300 of *IIb*, pages 41–44, 1985.

[12] P. Ladevèze. *Nonlinear Computational Structural Mechanics — New Approaches and Non-Incremental Methods of Calculation.* Springer Verlag, 1999.

[13] P. Ladevèze and D. Dureisseix. A micro / macro approach for parallel computing of heterogeneous structures. *International Journal for Computational Civil and Structural Engineering*, 1:18–28, 2000.

[14] R. W. Lewis, B. A. Schrefler, and L. Simoni. Coupling versus uncoupling in soil consolidation. *International Journal for Numerical and Analytical Methods in Geomechanics*, 15:533–548, 1991.

[15] R. Matteazzi, B. Schrefler, and R. Vitaliani. *Comparisons of partitioned solution procedures for transient coupled problems in sequential and parallel processing*, pages 351–357. Advances in Computational Structures Technology. Civil-Comp Ltd, 1996.

[16] R. Ohayon and J.-P. Morand. *Fluid-Structure Interaction: Applied Numerical Methods.* John Wiley & Sons, 1995.

[17] K. C. Park. Stabilization of partitioned solution procedure for pore fluid-soil interaction analysis. *International Journal for Numerical Methods in Engineering*, 19:1669–1673, 1983.

[18] S. Piperno, C. Farhat, and B. Larrouturou. Partitioned procedures for the transient solution of coupled aeroelastic problems. Part I: model problem, theory and two-dimensional application. *Computer Methods in Applied Mechanics and Engineering*, 124:79–112, 1995.

[19] Y. Saad. *Iterative methods for sparse linear systems.* PWS Publishing, 1996.

[20] A. V. Saetta and R. V. Vitaliani. Unconditionally convergent partitioned solution procedure for dynamic coupled mechanical systems. *International Journal for Numerical Methods in Engineering*, 33:1975–1996, 1992.

[21] B. A. Schrefler and R. W. Lewis. *The Finite Element Method in the Static and Dynamic Deformation and Consolidation of Porous Media.* Wiley, 2nd edition, 1998.

[22] E. Turska and B. A. Schrefler. On convergence conditions of partitioned solution procedures for consolidation problems. *Computer Methods in Applied Mechanics and Engineering*, 106:51–63, 1993.

[23] P. Verpeaux, T. Charras, and A. Millard. CASTEM 2000 : une approche moderne du calcul des structures. In J.-M. Fouet, P. Ladevèze, and R. Ohayon, editors, *Calcul des Structures et Intelligence Artificielle*, volume 2, pages 261–271. Pluralis, 1988.

[24] O. C. Zienkiewicz, D. K. Paul, and A. H. C. Chan. Unconditionally stable staggered solution procedure for soil-pore fluid interaction problems. *International Journal for Numerical Methods in Engineering*, 26:1039–1055, 1988.

[25] O. C. Zienkiewicz, S. Qu, R. L. Taylor, and S. Nakazawa. The patch test for mixed formulations. *International Journal for Numerical Methods in Engineering*, 23:1873–1883, 1986.

[26] O. C. Zienkiewicz and R. L. Taylor. *The finite element method.* Butterworth Heinemann, 5th edition, 2000.